RSC Advances

PAPER

View Article Online
View Journal | View Issue

Cite this: *RSC Adv.*, 2020, **10**, 18565

Hydrophobic mesoporous silicon dioxide for improving foam stability

Lihui Meng,[a] Qingwang Liu,*[a] Jigang Wang,[a] Zhenzhong Fan[a] and Xiaoming Wei[b]

Received 7th March 2020
Accepted 24th April 2020

DOI: 10.1039/d0ra02161j

rsc.li/rsc-advances

In this study, mesoporous SiO_2 nanoparticles (MSNs) were synthesized *via* a sol–gel method and modified with (3-chloropropyl) trimethoxysilane to make them hydrophobic (MMSNs). The material was characterized *via* SEM, TEM, FT-IR, DLS, BET and contact angle measurements. The MMSNs have good foam stability, so that the foam properties of the added particles have been increased by 38.4% in an oil/SDS solution. Simultaneously, it becomes a promising material for foam stabilization in order to enhance the oil recovery because it is bio-compatibile and environment friendly. Also, it provides a novel application-stable foam for mesoporous materials.

1 Introduction

In addition to the wide applications in the areas of plastics, papermaking, paints, batteries, medicine and food, nanoparticles have been widely used in the petroleum industry in recent years. Nanoparticles have been used as the main materials for enhancing oil recovery (EOR)[1] and can be used in foam flooding to stabilize unstable foams.

The destabilization of foams is controlled by three main mechanisms, such as the liquid drainage, gas diffusion through aqueous films and the coalescence of adjacent bubbles. Simultaneously, crude oil has an adverse effect on foam formation. First of all, surfactants have hydrophilic and oil-friendly groups, which are preferentially distributed at the oil–water interface. As a result, the concentration of surfactants at the gas–water interface decreases and the foam stability becomes worse. Second, the spread of the crude oil on the foam film produces a Marangoni effect, which thins or bursts the film.

In response to these problems, nanoparticles have numerous advantages in stabilizing foams, such as particle attachment energy, particle arrangement during film drainage, growing aggregate and cork formation and maximum capillary pressure of coalescence.[2] Most of the recent researches on foam flooding have focused on the use of nanoparticles as foaming additives. So, nanoparticles not only exhibit higher long-term stability, but also are designed to be biocompatible and environmentally friendly.[3,4] Numerous scholars use a single class of nanoparticles to stabilize foams such as modified SiO_2 nanoparticles, $CaCO_3$ nanoparticles, and Fe_3O_4 nanoparticles.[5–8]

Binks *et al.* observed the adsorption of a cationic surfactant, namely CTAB, on the negatively charged surface of solid particles and investigated the synergistic stabilization of modified solid particles on foam and emulsion. They found that the foam stability was enhanced by the adsorption of solid particles at the air/water interface and the formation of particle coagulation in the bulk phase. The maximum foam stability reached when the contact angle was close to 90°.[9,10]

Mesoporous silica nanoparticles (MSNs) have attracted a tremendous amount of attention in recent years due to their unique properties of large specific surface area and pore volume, low density, facile surface functionalization and excellent biocompatibility. All of these intrinsic properties make MSNs ideal candidates for numerous potential applications such as catalysis, separation, and drug delivery. For the first time, we have used mesoporous nanoparticles for stabilizing foams. They not only have the advantages of traditional solid nanoparticles, but also can achieve a better foam stabilization performance with the advantage of having an ultra-low density.

2 Experimental

2.1 Chemicals and materials

Diethanolamine (DEA), cetyltrimethylammonium bromide (CTAB), ethyl orthosilicate (TEOS), sodium dodecyl sulfate (SDS) and (3-chloropropyl) trimethoxysilane (CPTMO) were purchased from Aladdin Chemical Reagent Corporation. Anhydrous ethyl alcohol, distilled water and ammonium hydroxide. All of the reagents were used as received and without further purification.

2.2 Synthesis of the mesoporous SiO_2 nanoparticles

All the mesoporous particles were prepared *via* a sol–gel method.[11] The direct preparation of mesoporous SiO_2 was as follows: a certain amount of CTAB was added to 200 mL of distilled water at 90 °C in a water-bath heating for 10 min. The

[a]*Key Laboratory of Improving Oil Recovery by Ministry of Education, Northeast Petroleum University, Daqing, Heilongjiang, 163111, China. E-mail: liuqingwang@163.com*

[b]*National Energy Research and Development Center of Heavy Oil, Panjin, Liaoning, 124000, China*

pH of the solution was adjusted to 10 with DEA. After 15 min, a certain amount of TEOS diluted in ethanol was added to the solution. After centrifugation the final mesoporous SiO_2 was washed with absolute ethyl alcohol and dried at 60 °C for 12 h. Nano mesoporous SiO_2 was calcined to 500 °C by raising the temperature at a speed of 2 °C min^{-1}.

2.3 Surface modification of mesoporous SiO_2

The mesoporous SiO_2 nanoparticles were modified using (3-chloropropyl) trimethoxysilane (CPTMO). In this process, a solution of 0.5–3 vol% of CPTMO was prepared by adding anhydrous ethyl alcohol into an aqueous solution of SiO_2. The solution pH was adjusted to 10 using ammonia. The solution was vigorously stirred for 2 h at 50 °C, followed by centrifugation and drying to obtain the surface-modified mesoporous SiO_2 nanoparticles (MMSNs).

2.4 Characterization techniques

Scanning electron microscopy (SEM) was performed using a SUPRA 40 field emission scanning electron microscope (Carl Zeiss SMT AG, Germany) at two magnifications (*viz.* 36.81 k× and 150 k×) at an acceleration voltage of 5 kV. The size and shape of the particles were estimated *via* transmission electron microscopy (TEM) (JEOL JEM-1011). Nanoparticles were dispersed in anhydrous ethyl alcohol. A drop of the dispersion was placed on a copper mesh previously coated with carbon. The size distribution of the nanoparticles was measured *via* dynamic light scattering (DLS) using a BI-200SM multi-angle dynamic/static laser scattering instrument (Brookhaven, USA). Fourier transform infrared (FT-IR) spectroscopy was performed using a Thermo Scientific Nicolet 6700 FT-IR instrument within the scan range of 4000–400 cm^{-1}. The wettability tests were done by contact angle measurements with distilled water using a JY-PHb Automated Goniometer and the sessile drop method. N_2 sorption measurements of the samples were performed on an NVOA 2000e automatic gas adsorption instrument (Canta, USA). The samples were degassed at 200 °C overnight before the measurement. The surface area was calculated based on the Brunauer–Emmett–Teller (BET) model.

2.5 Preparation and characterization of aqueous foams

A certain mass of mesoporous SiO_2 nanoparticles was initially dispersed in a surfactant solution (100 mL of pure SDS solution or a mixed solution of 10 mL crude oil and 90 mL SDS solution; the viscosity of the crude oil is 100 mPa s) and the solution was dispersed with ultrasonic waves. Then, 100 cm^3 of the dispersion were transferred to an 800 cm^3 stirring cup and stirred at a high speed mixer for 2 min. The volume of the foam produced was transferred to a 1000 cm^3 cylinder and stored. The initial foam volume was taken as a measure of the foamability. The foam and liquid half-lives were taken as measures of the foam stability.[12]

3 Results and discussion

For the synthesis of mesoporous SiO_2 nanoparticles (MSNs), a typical sol–gel method was used with CTAB as the template to generate a template-driven synthesis, and TEOS was used as the silica resource. A possible formation mechanism for MSNs templated by CTAB was proposed (Fig. 1). When TEOS molecules are added, they consecutively hydrolyze and self-assemble with CTAB, resulting in the growth of silica on the surface of the micelles. After the removal of CTAB by calcination, the mesoporous silica nanoparticles are obtained.

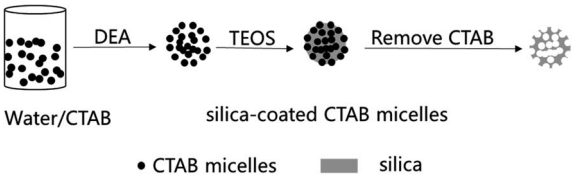

Fig. 1 Schematic of the formation of MSNs.

It is known that the surfactant (CTAB) is a critical additive in the formation of MSNs. TEOS cannot self-assemble to form MSNs without CTAB micelles. Under the conditions of heating in a water bath at 90 °C and a pH of 10, the micelle formation of CTAB was measured *via* a conductivity method, as shown in Fig. 2. Simultaneously, in order to control the morphology, the CTAB addition is controlled between the first critical micelle concentration (CMC1) and the second critical micelle concentration (CMC2) throughout the experiment. As shown in Fig. 2, CTAB reached the CMC1 at 1.4 mmol L^{-1} and remained in the same state before reaching 3 mmol L^{-1}. Therefore, in order to obtain stable spherical micelles, 2 mmol L^{-1} (0.146 g) was selected as the ideal experimental concentration of CTAB.

Previous studies have shown that the particle sizes of MSNs can be easily controlled by changing the amount of TEOS and the reaction times.[13–15] The particle size in Fig. 3a shows that when the amount of TEOS increased from 0.5 mL to 2 mL, the diameter of the MSNs increased from 30 nm to 51 nm.

The amount of TEOS has a great impact on the synthesis of MSNs, too much or too little will lead to an uneven particle size. When the amount of TEOS is less than 1 mL, the hydrolysis rate will be too fast because of the high dilution conditions, and it will not be able to deposit on the surface of the CTAB micelles neither self-aggregate to form particles larger than 40 nm.

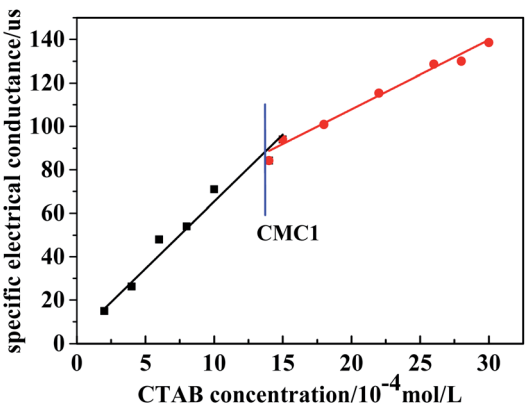

Fig. 2 Conductivity *versus* surfactant concentration.

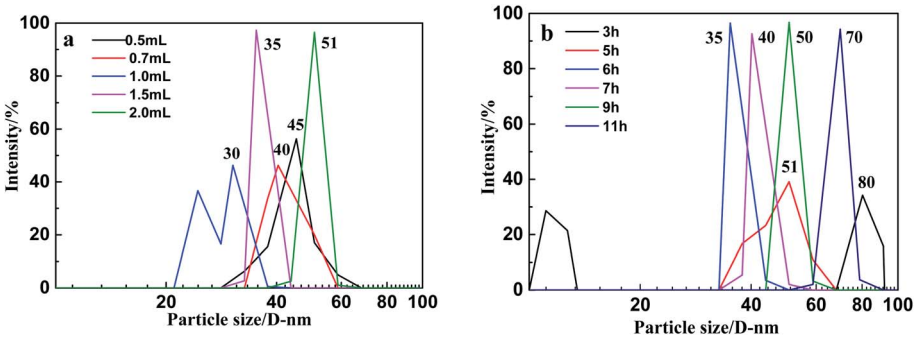

Fig. 3 The particle size of MSNs at (a) different amounts of TEOS (b) different reaction times.

However, when its concentration increases, the silica sol hydrolyzed by TEOS is directionally adsorbed onto the agglomerates in between the particles and breaks to form particles with a good dispersibility. When the amount of TEOS is 1.5 mL, the particle size is 35 nm. When the amount of TEOS continues to increase, a large amount of TEOS is hydrolyzed to form adhesions, resulting in the particle distribution and unevenness.

The particle size in Fig. 3b show that when the reaction time increased from 3 h to 11 h, the diameter of the MSNs increased from 35 nm to 80 nm (Fig. 3b). The particle size at the reaction time of 3 h is larger than that of the reaction time of 5 h, mainly because TEOS is not completely hydrolyzed at 3 h, and the partially hydrolyzed silica sol cannot form complete aggregates on the CTAB micelles. The agglomeration between them formed larger particles with a main particle diameter of 80 nm. When the reaction time is extended to 5 h, although the particle size is smaller than that during the 3 h reaction, the reaction system is not very stable, which results in a wide range of sizes for the synthetic particles, resulting in unevenness with a main particle size distribution located between 40 nm and 60 nm. When the reaction time was extended to 6 h, the concentration of TEOS gradually decreased, and the rate of the hydrolysis-polymerization also slowed down, thereby forming a more stable system with a uniform particle size of 35 nm. When the reaction time continues to increase, the particle size of the as-

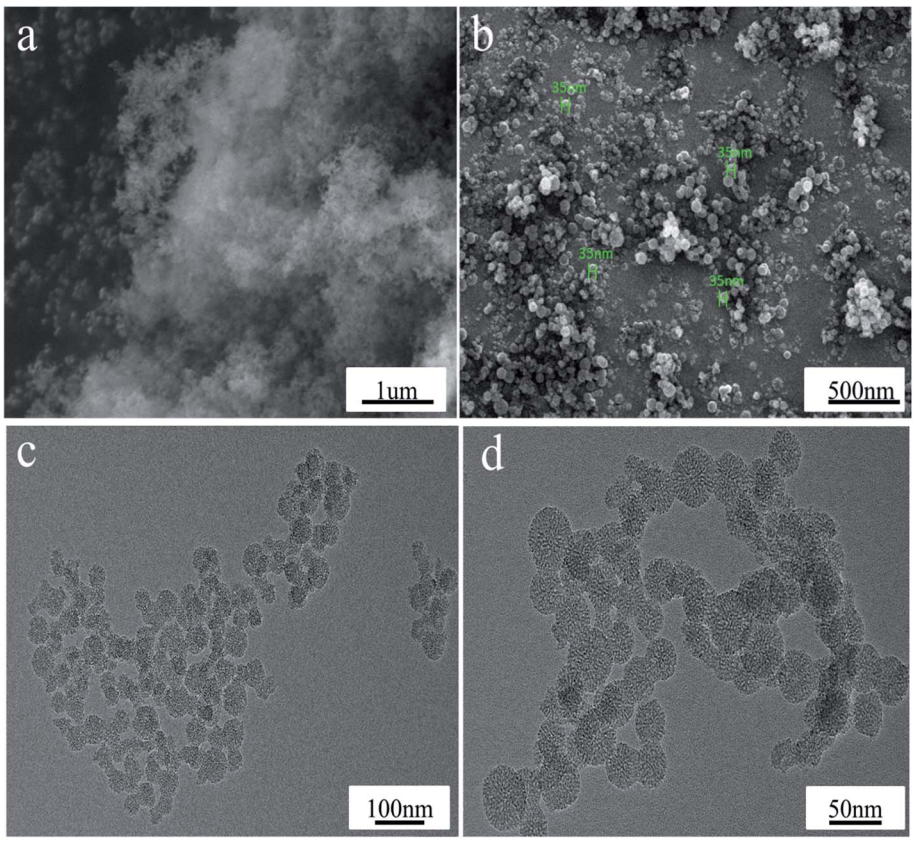

Fig. 4 SEM/TEM image of MSNs: (a) and (b), SEM; (c) and (d), TEM.

synthesized nanoparticles is relatively uniform, but the main particle size increases with the increase in the reaction time. The results show that TEOS-1.5 mL and reaction times of 6 h are the best reaction conditions. The synthesis of MSNs was finished by calcination at 500 °C by increasing the temperature at 2 °C min^{-1} for 4 h.

The SEM images in Fig. 4a and b show that the as-prepared reasonably uniform MSN spheres, which are fabricated in the presence of 1.5 mL of TEOS, 0.146 g of CTAB and during a reaction time of 5 h, have a diameter size of *ca.* 35 nm. The TEM images in Fig. 4c and d show that the MSNs have good ordered mesoporous properties with a pore size of *ca.* 3–8 nm.

In addition, nitrogen adsorption and desorption[16] were used to analyze the MSN structure (Fig. 5). From the IV-type adsorption and desorption curve of N_2, the adsorption has increased rapidly in the low pressure state, which mainly comes from the micropore filling. When the pressure continues to rise, the adsorption amount appears. Simultaneously, based on the nitrogen adsorption and desorption curve, the ratio was calculated by BET: the specific surface area was 790 m^2 g^{-1}, and the pore volume was 400 cm^3 g^{-1} and the pore size distribution was 4.5 nm.

The coupling agent ($RSiX_3$) modification has the best modification effect on inorganic ultrafine powders with hydroxyl groups on the surface. The silica was modified using the CPTMO coupling agent, where the content of CPTMO was 0.78–0.93–1.08–1.22–2.35%, and the contact angles of MMSNs were 16–80–105–128–138° (Fig. 6), also named MMSNs-1, MMSNs-2, MMSNs-3, MMSNs-4 and MMSNs-5, respectively. During coupling, the –X group is first hydrolyzed to silanol, and then reacted with the hydroxyl groups on the surface of the inorganic ultrafine powder particles to form hydrogen bonds and condense into –SiO–M covalent bonds. In this process, the silanol groups in the silane molecules associate with each other and form a network structure. The film covers the surface of the particles and makes them hydrophobic. The FTIR-ATR spectra of (a) MSNs and (b) MMSNs are shown in Fig. 7. From curves (a), the peaks at 800 cm^{-1} and 460 cm^{-1} resulted from the symmetrical stretching vibration of the Si–O, while the peaks at

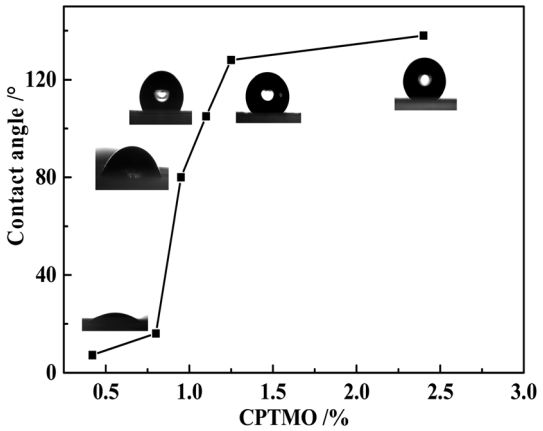

Fig. 6 Contact angle at different amounts of CPTMO.

1087 cm^{-1} resulted from the asymmetric Si–O–Si stretching. The strength of the absorption band at 3450 cm^{-1} corresponds to the stretch vibration of the –OH. The peak at 986 cm^{-1} is the Si–OH bending vibration. These results indicate that the as-prepared particles are silica particles. The peaks at 1540 cm^{-1} and 1648 cm^{-1} are characteristic of DEA, indicating that DEA not only provides alkaline conditions for the TEOS hydrolysis, but also participates in the reaction.[17] From the curves in (b), the peak at 698 cm^{-1} results from the stretching vibration of C–Cl and the peaks at 798 cm^{-1} and 1447 cm^{-1} result from the vibrations on the out-of-plane and in-plane deformations of the C–H group, respectively. The strength of the absorption band at 2953 cm^{-1} corresponds to the stretching vibration of $-CH_3$. This indicates that SiO_2 was modified by CPTMO successfully. Simultaneously, the stretching vibration of the O–H group at 3618 cm^{-1} shows the progress of the silanol hydrolyzed by CPTMO.

SDS can ionize surfactant anions in water. Such surfactants have excellent foaming properties, and are affordable and widely available.[18,19] It can be seen that when the SDS concentration is less than 0.0288 wt%, a stable foam is not produced.

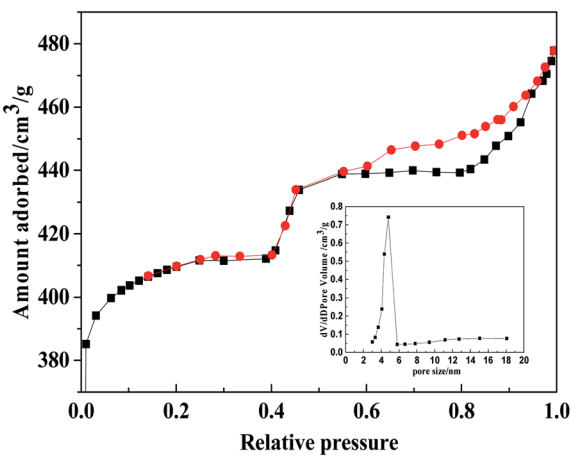

Fig. 5 The N_2-sorption isotherms of the MSNs.

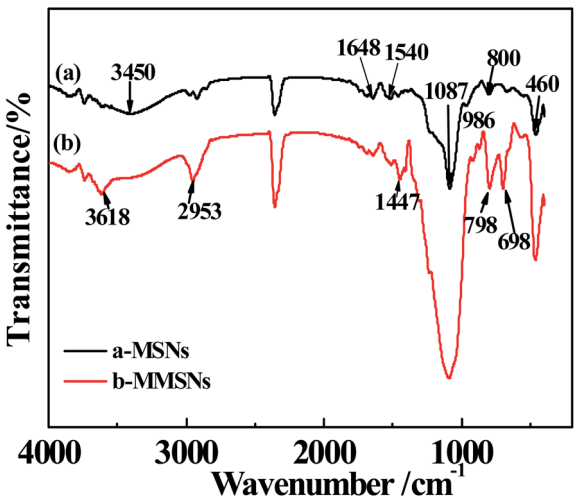

Fig. 7 FTIR spectra for (a) MSNs, (b) MMSNs.

Above this concentration, the foam volume increases steadily as the concentration of SDS increases. Even if the concentration of SDS is greater than 0.288 wt%, the foaming volume no longer increases significantly, and the half-decay time of the foam also remains unchanged at 418 s. Thus, 0.288 wt% of SDS is the optimum foaming agent concentration (Fig. 8).

Nanoparticles can be used as foam stabilizers to improve the foam stability. In the foaming system where the amount of surfactant is 0.288 wt%, adjusting the amount of the two kinds of solid particles, SiO_2 nanoparticles and MSNs (0.05 wt%, 0.10 wt%, 0.15 wt%, 0.20 wt%) leads to different foaming systems. The foam stability performance of the particles was tested and evaluated through the foaming experiment. The foam stabilization performance at different amounts of SiO_2 nanoparticles is shown in Fig. 9. The addition of nanoparticles will increase the foaming volume, but it is not obvious that the solid SiO_2 nanoparticles have increased the foam stabilization performance. However, the addition of solid SiO_2 nanoparticles in the system, shortens the liquid half-decay time, mainly because the contact angle of the nanoparticles is less than 30° (Illustration for the contact angle: solid SiO_2, 6° and MSNs, 6°), and the super-hydrophilic nanoparticles have no obvious foam stabilizing function. However, compared with the synthesis of MSNs, the liquid half-decay time did not appear to be shortened due to its ultra-low density. As the number of nanoparticles increase, the liquid half-decay time will become longer. The amount of nanoparticles at 0.1 wt% has the best foam stabilizing effect. Continuing to increase the amount of nanoparticles will worsen the foam stabilizing performance, mainly because the foaming system agglomerates into larger particles, which affects the foaming performance.

The volume of foam in a graduated cylinder is measured with 0.1 wt% MMSNs dispersed in 0.288 wt% SDS solution. The foam volume of the solution of MMSN particles is increasing compared with the pure SDS solution. The adsorption of SDS molecules between the MMSNs and the water interface produces a synergistic effect, meaning that the surface tension of the SiO_2/SDS foam system is lower than the surface tension of the pure SDS solution at the same concentration. At the

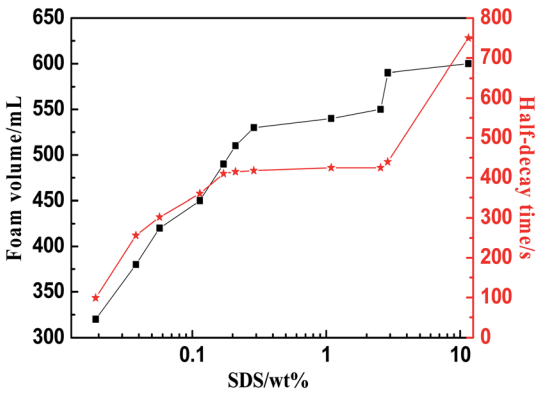

Fig. 8 Foam performance of SDS solutions at different concentrations.

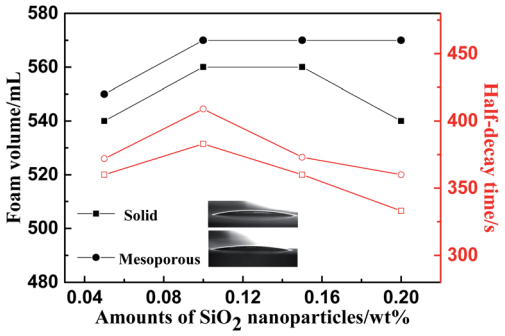

Fig. 9 Foam performance at different concentrations of SiO_2 nanoparticles.

appropriate SDS concentration, the surfactant molecules adsorbed onto the particle surface can enhance the surface activity and facilitate the adsorption of particles on the gas–liquid interface. However, MMSNs with different contact angles have different effects on the stability of the particles. The adsorption of surfactants on the surface of the particles has been extensively studied.[20–22] From the ion adsorption energy point of view, when the contact angle is lower than 30°, the adsorption energy is low and the nanoparticles cannot be stabilized. When the contact angle is around 90°, the adsorption energy is high and the bubble stabilization function is provided. Therefore, MMSNs-2 and MMSNs-3 were used for the foaming experiments in pure SDS solution or oil/SDS solution.

Compared with the foaming system without particles, the foam volume for the foaming system MMSNs-2 has increased, but the foam decay-time has improved significantly, and the overall foam properties increased up to 10.9% (Fig. 10a). Compared with the oil–water foaming system without particles, the foam decay-time for MMSNs-3 has improved significantly, and the foam properties increased up to 38.4%, effectively improving the foam's oil resistance (Fig. 10b).

Fig. 11 shows that the foam liquid film becomes thinner when the oil phase is added compared to the foam without the oil phase. Simultaneously, the oil phase (dispersed in aqueous phase as small droplets) will continue to move between the liquid films with the rupture of the foam. As the time increases, the oil phase will eventually concentrate and cause the foam to coarsen, rupture and eventually disappear. However, after adding MMSNs to the foam system, the nanoparticles are well dispersed between the liquid films and have a certain interface adsorption performance. The foam liquid film and membrane formed by the adsorption of the nanoparticles are tougher, have a better mechanical strength, and their foam stability is enhanced.

Compared with solid nanoparticles, MMSNs have a larger specific surface area and a lower density, which reduces the phenomenon of the quick rise of bubbles to the surface of liquids due to the difference in the gas–liquid density. Simultaneously, mesoporous particles enable a better adsorption of the surfactant in the foam liquid film, thereby enhancing the stability of the foam. The foam liquid film becomes thinner over time, and the size of the foam will increase, coarse and

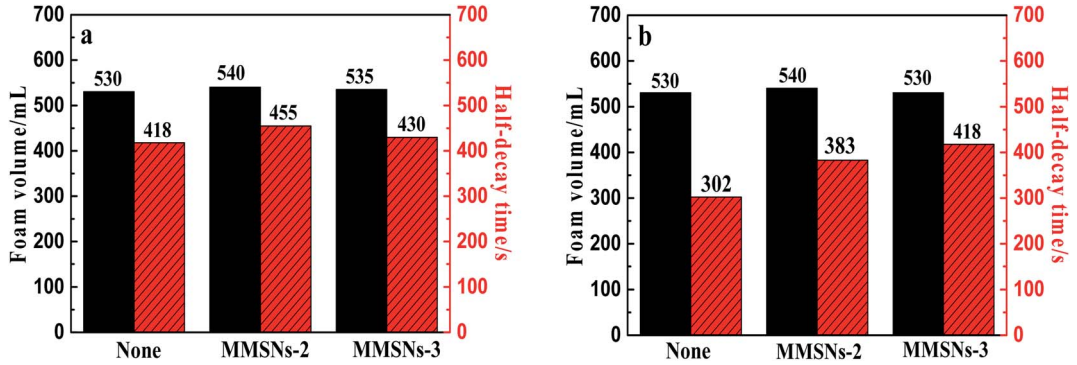

Fig. 10 Foam performance of (a) pure SDS solutions (b) oil/SDS solution with MMSNs.

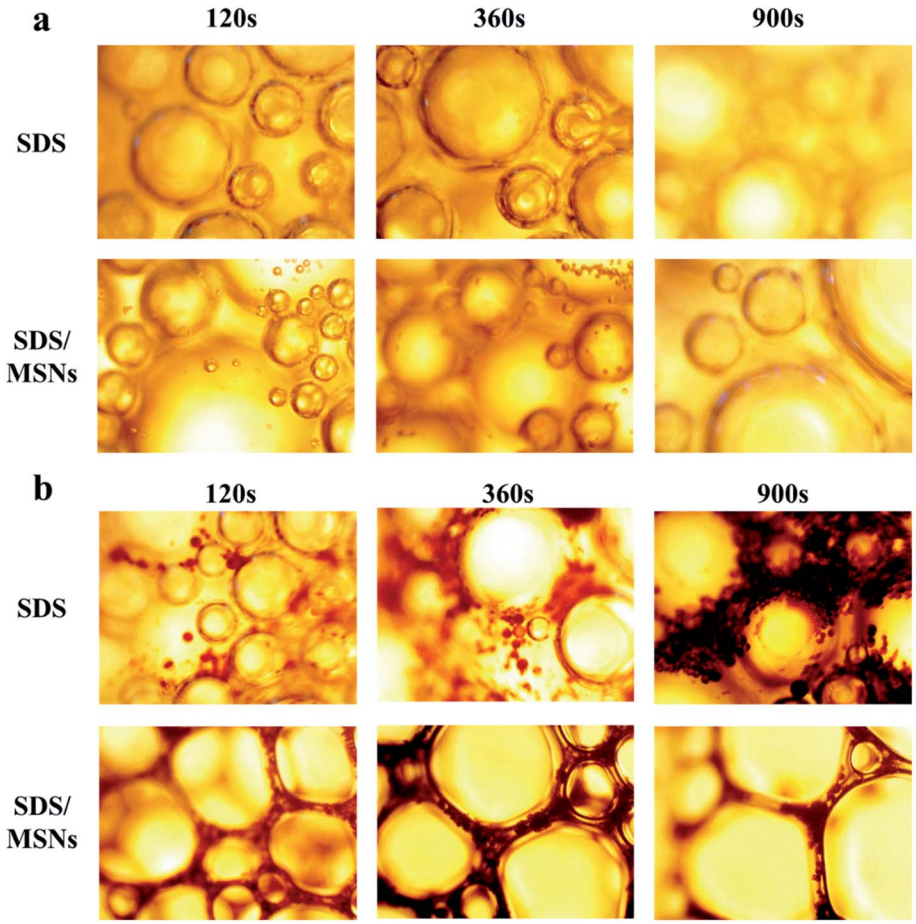

Fig. 11 Microscopic observation of the foam from (a) pure SDS solutions (b) oil/SDS solution.

eventually disappear. Under microscopic observation, the time for the liquid film to strengthen increases in the presence of MMSNs, which can maintain the stability of the foam for longer periods of time. Also, the surfactant molecules can be better maintained between the liquid films due to the presence of MMSNs, which reduces the foam rupture and enhances the resistance of the foam toward oil. Therefore, mesoporous SiO_2 nanoparticles have found a new application.

4 Conclusion

In summary, we adopted a sol–gel methodology for synthesizing mesoporous SiO_2 nanoparticles (MSNs) and modified them with (3-chloropropyl) trimethoxysilane to make them hydrophobic (MMSNs). The produced MMSNs have a good foam stability, so that the overall foam properties increased by 10.9% in pure SDS solution and 38.4% in an oil/SDS solution. MMSNs have a larger specific surface area and a lower density, which

reduces the differences in the gas–liquid density that result in the phenomenon of the quick rise of bubbles to the surface of the liquid. Simultaneously, the existence of pores on the particle surface enables the particles to adsorb well the surfactant in the foam liquid film, thereby enhancing the stability of the foam, and effectively improving the foam's resistance to oil. Moreover, it is a promising material for the stabilization of foams in order to enhance the oil recovery because of its biocompatibility and environment friendly character, providing a new application for mesoporous materials.

Disclosure statement

No potential conflict of interest was reported by the authors.

Conflicts of interest

There are no conflicts to declare.

Acknowledgements

The authors acknowledge the support from National Science and Technology Major Project-Research on Hot Air Foam Composite Flooding Technology after Steam Flooding, 2016ZX05002006.

References

1 X. Sun, Application of nanoparticles in enhanced oil recovery: a critical review of recent progress, *Energies*, 2017, **10**(3), 345.
2 H. Farhadi, S. Riahi, S. Ayatollahi and H. Ahmadi, Experimental study of nanoparticle-surfactant-stabilized co$_2$ foam: stability and mobility control, *Chem. Eng. Res. Des.*, 2016, **111**, 449–460.
3 J. Tang, P. J. Quinlan and K. C. Tam, Stimuli-responsive pickering emulsions: recent advances and potential applications, *Soft Matter*, 2015, **11**(18), 3512–3529.
4 N. Liu, Nanoparticle-stabilized CO_2 foam for CO_2 EOR application, *Final report*, Pittsburgh, National Energy Technology Laboratory, US Department of Energy, 2015 Apr.
5 Z. Alyousef, M. Almobarky and D. Schechter, Enhancing the Stability of Foam by the Use of Nanoparticles, *Energy Fuels*, 2017, **31**(10), 10620–10627.
6 Z. G. Cui, Y. Z. Cui, C. F. Cui, *et al.*, Aqueous foams stabilized by in situ surface activation of $CaCO_3$ nanoparticles via adsorption of anionic surfactant, *Langmuir*, 2010, **26**, 12567–12574.
7 S. Kovačič, B. N. Matsko, G. Ferk, *et al.*, Macroporous poly (dicyclopentadiene)$\gamma Fe_2O_3/Fe_3O_4$ nanocomposite foams by high internal phase emulsion templating, *J. Mater. Chem. A*, 2013, **1**(27), 7971–7978.
8 K. Jin, S. K. Bea, Y. H. Kim, D. W. Kim, K. Y. Lee and C. M. Lee, Improved suspension stability of calcium carbonate nanoparticles by surface modification with oleic acid and phospholipid, *Biotechnol. Bioprocess.*, 2015, **20**, 794–799.
9 B. P. Binks, M. Kirkland and J. A. Rodrigues, Origin of stabilisation of aqueous foams in nanoparticle–surfactant mixtures, *Soft Matter*, 2008, **4**, 2373–2382.
10 S. Zhang, Q. Lan, Q. Liu, *et al.*, Aqueous foams stabilized by Laponite and CTAB, *Colloids Surf., A*, 2008, **317**, 406–413.
11 N. I. Vazquez, Z. Gonzalez, B. Ferrari, *et al.*, Synthesis of mesoporous silica nanoparticles by sol–gel as nanocontainer for future drug delivery applications, *Bol. Soc. Esp. Ceram. Vidrio*, 2017, **56**(3), 139–145.
12 Z. Wang, G. Ren, J. Yang, *et al.*, CO_2-responsive aqueous foams stabilized by pseudogemini surfactants, *J. Colloid Interface Sci.*, 2019, **536**, 381–388.
13 Z. Feng, Y. Li, D. Niu, *et al.*, A facile route to hollow nanospheres of mesoporous silica with tunable size, *Chem. Commun.*, 2008, **23**, 2629–2631.
14 D. Niu, Z. Ma, Y. Li, *et al.*, Synthesis of core-shell structured dual-mesoporous silica spheres with tunable pore size and controllable shell thickness, *J. Am. Chem. Soc.*, 2010, **132**(43), 15144–15147.
15 X. Zhou, X. Cheng, W. Feng, *et al.*, Synthesis of hollow mesoporous silica nanoparticles with tunable shell thickness and pore size using amphiphilic block copolymers as core templates, *Dalton Trans.*, 2014, **43**(31), 11834–11842.
16 L. Sheng, Y. Zhang, F. Tang, *et al.*, Mesoporous/microporous silica materials: preparation from natural sands and highly efficient fixed-bed adsorption of methylene blue in wastewater, *Microporous Mesoporous Mater.*, 2018, **257**, 9–18.
17 J. Mo, L. He, B. Ma, *et al.*, Tailoring particle size of mesoporous silica nanosystem to antagonize glioblastoma and overcome blood-brain barrier, *ACS Appl. Mater. Interfaces*, 2016, **8**(11), 6811–6825.
18 M. Patowary, K. Pathak and R. Ananthakrishnan, A facile preparation of superhydrophobic and oleophilic precipitated calcium carbonate sorbent powder for oil spill clean-ups from water and land surfaces, *RSC Adv.*, 2015, **5**, 79852–79859.
19 N. I. Guanhua, X. Hongchao, L. I. Shang, *et al.*, The effect of anionic surfactant (SDS) on pore-fracture evolution of acidified coal and its significance for coalbed methane extraction, *Adv. Powder Technol.*, 2019, **30**(5), 940–951.
20 M. G. Chernysheva, A. G. Popov, V. N. Tashlitsky, *et al.*, Cationic surfactant coating nanodiamonds: Adsorption and peculiarities, *Colloids Surf., A*, 2019, **565**, 25–29.
21 A. M. Khan, F. Shafiq, S. A. Khan, *et al.*, Surface modification of colloidal silica particles using cationic surfactant and the resulting adsorption of dyes, *J. Mol. Liq.*, 2019, **274**, 673–680.
22 H. Vatanparast, A. Samiee and A. Bahramian, Surface behavior of hydrophilic silica nanoparticle-SDS surfactant solutions: I. Effect of nanoparticle concentration on foamability and foam stability, *Colloids Surf., A*, 2017, **513**, 430–441.